

## Optimum amount of additive mass in scaling of operational mode shapes

M.M. Khatibi, M.R. Ashory\* and A.R. Albooyeh

Modal Analysis Lab., School of Mechanical Engineering, Semnan University, Semnan 35195-363, Iran

(Received August 22, 2010, Accepted June 24, 2011)

**Abstract.** Recently, identification of modal parameters using the response only data has attracted considerable attention particularly where the classic modal testing methods is difficult to conduct. One drawback of the response only data, also known as Operational Modal Analysis (OMA), is that only the unscaled mode shapes can be obtained which restricts the applications of OMA. The Mass change method is a usual way to scale the operational mode shapes. In this article a new method is proposed to optimize the additive mass for scaling of the unscaled mode shapes from OMA for which a priori knowledge of the Finite Element model of structure is required. It is shown that the total error of the scaled mode shapes is minimized using the proposed method. The method is validated using a numerical case study of a beam. Moreover, the experimental results of a clamped-clamped beam demonstrate the applicability of the method.

**Keywords:** operational modal analysis; scaling; mode shapes; mass-change; sensitivity analysis

---

### 1. Introduction

The dynamic analysis of structures is one of the requirements for their design and maintenance. The Finite Element (FE) models of complex structures are not accurate enough due to the errors in the details of geometry, material properties and boundary conditions. Modal testing is known as an experimental alternative for modelling of the dynamic behaviour of complex structures. One drawback of the traditional modal testing is that the excitation of test structures such as the bridges and buildings are sometimes impossible or difficult to conduct. Also the dynamic behaviours of the structures such as cars, ships and bridges in-operation differ with their condition during a laboratory vibration test. The environmental noise may also contaminate the force as well as the response signals. In the past few years Operational Modal Analysis (OMA) methods have become a valid alternative for structures where the classic modal testing methods would be difficult to conduct. In OMA which is also known as Ambient Modal Analysis or Output-Only Modal Analysis (Zhang *et al.* 2005), only the response is measured and the test structure is excited by the ambient forces such as traffic, wind and waves. The first applications of OMA were reported for the suspending bridges (Abel-Ghaffer *et al.* 1978), and vibrating structures without much success (Begg *et al.* 1976, Wenzel *et al.* 2005). Recently more successful procedures have been reported (James *et al.* 1995, Asmussen

---

\*Corresponding author, Assistant Professor, E-mail: [mr.ashory@gmail.com](mailto:mr.ashory@gmail.com), [mashoori@semnan.ac.ir](mailto:mashoori@semnan.ac.ir)

*et al.* 1999, Hanson 2006, Brownjohn *et al.* 2010).

A disadvantage of OMA is that the mode shapes can not be scaled due to the fact that the ambient excitation can not be measured. The incompleteness of the modal parameters restricts its applicability in some important applications such as model updating, structural dynamic modification and response prediction. The scaling methods are separated into two categories. In the first group some extra data or some restrictions are required for the method. Doebling *et al.* (1996) used the FE model of structures for scaling the operational mode shapes. Randall *et al.* (1998) considered some limitations in the type of excitation for scaling procedure. Deweer *et al.* (1999) used the forced vibration test on some selected points on the structure in order to scale the operational mode shapes. In the second group the scaling is conducted using only the test data and by changing the stiffness of structure, the mass (Aenlle *et al.* 2005a) or both the mass and stiffness (Coppotelli 2009, Khatibi *et al.* 2009). The ambient test is repeated and the scaling factors are estimated by comparing the results (Aenlle *et al.* 2005a).

The mass change method was first proposed by Parloo *et al.* (2002) based on the modal sensitivity equations. Brincker *et al.* (2003) proposed an alternative expression derived from the eigen-value equations and the assumption of negligible changes in the mode shapes. Also, additional expressions derived from the eigen-value equations using both the modified and original mode shapes (Aenlle *et al.* 2005a, b). A different formulation of the mass change method has been proposed by Bernal (2004) for the cases where the changes in the mode shapes are not negligible. The projection of the modified mode shape in the original one is used to improve the estimated scaling factors.

A suitable mass change strategy is required in order to scale the mode shapes accurately in which the magnitude, the location and the number of additive masses have to be determined. Such a mass change strategy was proposed by Aenlle *et al.* (2010), who demonstrated that the accuracy of the scaling factors depends on both the accuracy of the identified modal parameter and the mass change strategy. However, he could not present an explicit formula for selecting the magnitude of additive mass. In this paper, a new method is proposed for selection of additive masses in scaling of operational mode shapes in order to minimize the scaling error. The FE model of structure is required to perform the sensitivity analysis in order to select the optimum extra masses for minimizing the scaling error. A numerical case study is used to demonstrate the effectiveness of the new formula. Also, the method is validated experimentally by testing a clamped-clamped beam.

## 2. Theory

### 2.1 Frequency Domain Decomposition (FDD) method

The OMA methods may be categorized into: time domain methods and frequency domain methods (Hanson 2006). On the other hand, these methods may be separated into parametric and non-parametric methods (Hanson 2006). The Frequency Domain Decomposition (FDD) method is a non-parametric frequency domain technique which was first proposed in (Brincker *et al.* 2000, 2001b). In this method, the Power Spectral Density (PSD) of the response is computed and the singular value decomposition is performed to obtain the modal parameters of system including the unscaled mode shapes. The relation between the inputs and outputs is given by Brincker *et al.* (2001a)

$$[G_{yy}(j\omega)] = [\bar{H}(j\omega)][G_{xx}(j\omega)][H(j\omega)]^t \tag{1}$$

where  $G_{xx}$  is the Power Spectral Density (PSD) matrix of input,  $G_{yy}$  is the PSD matrix of output,  $[H(j\omega)]$  is the FRF matrix, the superscript “ $t$ ” indicates the transpose of the matrix, the superscript “ $-$ ” indicates the complex conjugate of the matrix and  $j$  is equal to  $\sqrt{-1}$ . If the input force is assumed to be a white signal, the PSD matrix of the output can be given by

$$[G_{yy}(j\omega)] = \sum_{k=1}^n \left( \frac{d_k \{\psi_k\} \{\psi_k\}^t}{j\omega - \lambda_k} + \frac{\bar{d}_k \{\bar{\psi}_k\} \{\bar{\psi}_k\}^t}{j\omega - \bar{\lambda}_k} \right) \tag{2}$$

where  $d_k$  is a scalar,  $\{\psi_k\}$  is the  $k^{\text{th}}$  unscaled mode shape vector,  $\lambda_k$  is the  $k^{\text{th}}$  complex resonance frequency and  $n$  is the number of modes.

The PSD of the response in each frequency can be decomposed to the singular-values and singular-vectors using the following equation

$$[G_{yy}(j\omega_i)] = [U_i][S_i][U_i]^H \tag{3}$$

where  $[U_i]$  is the  $i^{\text{th}}$  singular-vectors matrix,  $[S_i]$  is the  $i^{\text{th}}$  singular-values matrix,  $\omega_i$  is the  $i^{\text{th}}$  frequency and “ $H$ ” indicates the complex conjugate and transpose of a matrix.

As the singular-values are directly related to modal participation factors, the number of non-zero singular-values indicates the number of modes which contribute the response of system at that frequency. The peaks of first singular values of system correspond to the natural frequencies of system. The singular-vectors corresponding to the peaks of the first singular-values estimate the mode shapes. The half power point method has been applied to estimate the damping ratios without much success (Brincker *et al.* 2001a).

### 2.2 Mass change method

The mode shapes obtained from OMA are not scaled; therefore an additional method is required to estimate the scaling factor of mode shapes. In traditional modal testing, the mode shapes are assumed to be orthogonal with respect to the mass matrix, i.e., (Ewins 2000)

$$\{\phi\}^t [M] \{\phi\} = 1 \tag{4}$$

where  $\{\phi\}$  is the scaled mode shape vector from traditional modal testing and  $[M]$  is the mass matrix. However, the unscaled mode shapes from OMA do not satisfy the equation

$$\{\psi\}^t [M] \{\psi\} = 1 \tag{5}$$

where  $\{\psi\}$  is the unscaled mode shape vector. The relation between the unscaled mode shape vector  $\{\psi\}$  and the scaled mode shape vector  $\{\phi\}$  is

$$\{\phi\} = \frac{\{\psi\}}{\sqrt{\{\psi\}^t [M] \{\psi\}}} \tag{6}$$

Therefore, the scaling factors can be estimated by the following equation

$$\alpha = \frac{1}{\sqrt{\{\psi\}^t [M] \{\psi\}}} \quad (7)$$

where  $\alpha$  is the scaling factor and

$$\{\phi\} = \alpha \{\psi\} \quad (8)$$

If the mass matrix is known, Eq. (7) can be used to scale the mode shapes. However, the mass matrix can not be estimated accurately for real structures.

The classic eigen-value problem for an undamped system or a system with proportional damping is

$$[M] \{\phi_1\} \omega_{n1}^2 = [K] \{\phi_1\} \quad (9)$$

where  $[K]$  is the stiffness matrix,  $\{\phi_1\}$  the scaled mode shape vector for the original structure and  $\omega_{n1}$  is the corresponding natural frequency. If the distribution of mass is changed, the new eigenvalue problem becomes

$$([M] + [\Delta M]) \{\phi_2\} \omega_{n2}^2 = [K] \{\phi_2\} \quad (10)$$

where  $[\Delta M]$  is the mass change matrix,  $\{\phi_2\}$  is the scaled mode shape vector after mass change and  $\omega_{n2}$  is the corresponding natural frequency.

The mass change is assumed to be so small that the mode shape vectors before and after mass change are almost the same; i.e., (Brincker *et al.* 2003)

$$\{\phi_2\} \cong \{\phi_1\} = \{\phi\} \quad (11)$$

By combining Eqs. (9), (10) and (11), the following equation is obtained

$$[M] \{\phi\} (\omega_{n1}^2 - \omega_{n2}^2) = [\Delta M] \{\phi\} \omega_{n2}^2 \quad (12)$$

Pre-multiplying Eq. (12) by  $\{\phi\}^t$  and considering the orthogonality of modes and by substituting Eq. (8) into Eq. (12), the scaling factor can be estimated as (Brincker *et al.* 2003)

$$\alpha = \sqrt{\frac{(\omega_{n1}^2 - \omega_{n2}^2)}{\omega_{n2}^2 \{\psi\}^t [\Delta M] \{\psi\}}} \quad (13)$$

Both the unscaled mode shapes before mass change or after mass change may be used in Eq. (13). Also, the mode shapes may be normalized to the length or to unity. It is shown in (Aenlle *et al.* 2005a, b) that the best results are obtained when the mode shapes are scaled to the length and both the modified and unmodified mode shapes are used in Eq. (13) which is given by the equation

$$\alpha_{12} = \sqrt{\frac{(\omega_{n1}^2 - \omega_{n2}^2)}{\omega_{n2}^2 \{\psi_1\}^t [\Delta M] \{\psi_2\}}} \quad (14)$$

where  $\{\psi_1\}$  and  $\{\psi_2\}$  are the unscaled mode shapes before and after mass change.

### 2.3 Optimized scaling of mode shapes

The novelty of this paper is essentially to estimate the magnitude of mass change in order to minimize the error of scaling. The method is based on the results of the Finite Element model of structure. The error of scaling as proposed in (Parloo 2003) can be given by

$$MSF_i = \frac{\{\varphi\}_{S-i}^t \{\varphi\}_{S-i}}{\{\varphi\}_{F-i}^t \{\varphi\}_{F-i}} \quad (15)$$

where  $\{\varphi\}_{S-i}$  is the scaled mode shape including only the translational DOFs,  $\{\varphi\}_{F-i}$  is the FE mode shape including only the translational DOFs and MSF stands for the Modal Scaling Factor. Here, only the translational DOFs are considered because there are not efficient methods and devices to measure the rotational degrees of freedom (Ewins 2000).

If MSF is equal to one, the scaled mode shapes are completely correlated to the FE mode shapes. Therefore, the error of scaling can be defined by the following equation

$$E_i = |1 - MSF_i| \quad (16)$$

For  $N$  modes of structure, the average of error can be given by

$$E_{ave.} = \frac{1}{N} \sum_{i=1}^N E_i \quad (17)$$

By substituting Eqs. (8), (15) and (16) in Eq. (17) the following equation is obtained

$$E_{ave.} = \frac{1}{N} \sum_{i=1}^N \left| 1 - \alpha_i^2 \frac{\{\psi\}_i^t \{\psi\}_i}{\{\varphi\}_{F-i}^t \{\varphi\}_{F-i}} \right| \quad (18)$$

where  $\alpha_i$  is the  $i^{\text{th}}$  scaling factor and  $\{\psi\}_i$  is the  $i^{\text{th}}$  unscaled mode shape. By substituting Eq. (13) in Eq. (18), the average error of scaling is given by

$$E_{ave.} = \frac{1}{N} \sum_{i=1}^N \left| 1 - \frac{\omega_{i1}^2 - \omega_{i2}^2}{\omega_{i2}^2 \{\psi\}_i^t [\Delta M] \{\psi\}_i} \times \frac{\{\psi\}_i^t \{\psi\}_i}{\{\varphi\}_{F-i}^t \{\varphi\}_{F-i}} \right| \quad (19)$$

If we assume that the equal masses are added to the structure at all its translational degrees of freedom. The mass change matrix reduces to

$$[\Delta M] = \Delta m [I] \quad (20)$$

By substituting Eq. (20) into Eq. (19) and considering the relation  $\{\psi\}_i^t [I] \{\psi\}_i = \{\psi\}_i^t \{\psi\}_i$ , Eq. (19) is simplified to

$$E_{ave.} = \frac{1}{N} \sum_{i=1}^N \left| 1 + \frac{A_i}{\Delta m} - \frac{A_i \omega_{i1}^2}{\Delta m \omega_{i2}^2} \right| \quad (21)$$

In which

$$A_i = \frac{1}{\{\varphi\}_{F-i}^t \{\varphi\}_{F-i}} \quad (22)$$

The following equation can be concluded from Eq. (21) using the elementary algebra

$$\frac{1}{N} \sum_{i=1}^N \left| 1 + \frac{A_i}{\Delta m} - \frac{A_i \omega_{i1}^2}{\Delta m \omega_{i2}^2} \right| \leq \frac{1}{N} \sum_{i=1}^N |1| + \frac{1}{N} \sum_{i=1}^N \left| \frac{A_i}{\Delta m} \right| + \frac{1}{N} \sum_{i=1}^N \left| -\frac{A_i \omega_{i1}^2}{\Delta m \omega_{i2}^2} \right| \quad (23)$$

Therefore

$$E_{ave.} \leq 1 + \frac{1}{N \Delta m} \sum_{i=1}^N A_i + \frac{1}{N \Delta m} \sum_{i=1}^N \frac{A_i \omega_{i1}^2}{\omega_{i2}^2} \quad (24)$$

It is clear that  $E_{ave.}$  is reduced by minimizing the right hand side of Eq. (24). It can be concluded that  $E_{ave.}$  is reduced when

$$\frac{\partial}{\partial \Delta m} \left( 1 + \frac{1}{N \Delta m} \sum_{i=1}^N A_i + \frac{1}{N \Delta m} \sum_{i=1}^N \frac{A_i \omega_{i1}^2}{\omega_{i2}^2} \right) = 0 \quad (25)$$

or

$$-\frac{B}{\Delta m^2} - \frac{1}{N \Delta m^2} \sum_{i=1}^N \frac{A_i \omega_{i1}^2}{\omega_{i2}^2} + \frac{1}{N \Delta m} \frac{\partial}{\partial \Delta m} \left( \sum_{i=1}^N \frac{A_i \omega_{i1}^2}{\omega_{i2}^2} \right) = 0 \quad (26)$$

where

$$B = \frac{1}{N} \sum_{i=1}^N A_i \quad (27)$$

Eq. (26) can be simplified to

$$\frac{B}{\Delta m} = -\frac{1}{N \Delta m} \sum_{i=1}^N \frac{A_i \omega_{i1}^2}{\omega_{i2}^2} + \frac{1}{N} \sum_{i=1}^N \left( \frac{-A_i \omega_{i1}^2}{\omega_{i2}^4} \times \frac{\partial \omega_{i2}^2}{\partial \Delta m} \right) \quad (28)$$

The derivative part in Eq. (28) can be simplified to

$$\frac{\partial \omega_{i2}^2}{\partial \Delta m} = 2 \omega_{i2} \frac{\partial \omega_{i2}}{\partial \Delta m} \quad (29)$$

If the structure is linear, the total change of natural frequency is equal to change of natural frequency due to each additive mass. Therefore the derivative part in the right hand-side of Eq. (29) can be simplified to (Parloo *et al.* 2002)

$$\frac{\partial \omega_{i2}}{\partial \Delta m} = \sum_{k=1}^L \frac{\partial \omega_{i2}}{\partial m_k} \quad (30)$$

where  $m_k$  is the mass change at the  $k^{\text{th}}$  DOF and  $L$  is the number of translational DOFs.

The sensitivity of the natural frequency of the  $i^{\text{th}}$  mode,  $\omega_i$ , to the mass change at the  $k^{\text{th}}$  DOF,  $m_k$ , as derived by Parloo *et al.* (2002) can be given by

$$\frac{\partial \omega_i}{\partial m_k} = -\omega_i \frac{\phi_{ki}^2}{2} \quad (31)$$

where  $\phi_{ki}$  is the  $k^{\text{th}}$  element of the  $i^{\text{th}}$  FE mode shape. Consequently, by Combining Eqs. (29), (30) and (31), the following equation can be obtained

$$\frac{\partial \omega_{i2}^2}{\partial \Delta m} = 2\omega_{i2} \sum_{k=1}^L -\omega_{i2} \frac{\phi_{ki}^2}{2} \tag{32}$$

On the other hand the relation between the natural frequency after mass change and the natural frequency before mass change can be given by

$$\omega_{i2} = \omega_{i1} + \frac{\partial \omega_{i1}}{\partial \Delta m} = \omega_{i1} + \sum_{k=1}^L -\omega_{i1} \frac{\phi_{ki}^2}{2} \tag{33}$$

By substituting Eq. (33) in Eq. (32), the following equation is obtained

$$\frac{\partial \omega_{i2}^2}{\partial \Delta m} = 2 \left( \omega_{i1} + \sum_{k=1}^L -\omega_{i1} \frac{\phi_{ki}^2}{2} \right) \times \sum_{k=1}^L - \left( \omega_{i1} + \sum_{k=1}^L -\omega_{i1} \frac{\phi_{ki}^2}{2} \right) \frac{\phi_{ki}^2}{2} \tag{34}$$

Combining Eqs. (28), (33) and (34) yields

$$\Delta m = \frac{B + \frac{1}{N} \sum_{k=1}^N \frac{A_i \omega_{i1}^2}{\left( \omega_{i1} + \sum_{k=1}^L -\omega_{i1} \frac{\phi_{ki}^2}{2} \right)^2}}{\frac{1}{N} \sum_{i=1}^N \frac{-A_i \omega_{i1}^2}{\left( \omega_{i1} + \sum_{k=1}^L -\omega_{i1} \frac{\phi_{ki}^2}{2} \right)^4} \times 2 \left( \omega_{i1} + \sum_{k=1}^L -\omega_{i1} \frac{\phi_{ki}^2}{2} \right) \times \sum_{k=1}^L - \left( \omega_{i1} + \sum_{k=1}^L -\omega_{i1} \frac{\phi_{ki}^2}{2} \right) \frac{\phi_{ki}^2}{2}} \tag{35}$$

Eq. (35) gives the optimum mass change for scaling of the mode shapes obtained from OMA methods.  $A_i$  is given by Eq. (22),  $\omega_{i1}$  and  $\phi_{ki}$  can be obtained from the initial FE analysis of the structure or the other numerical methods.

### 3. Simulation

#### 3.1 Finite element model of a clamped-clamped beam

The Finite Element Method (FEM) was used for estimating of the natural frequencies and mode shapes of a clamped-clamped beam (Fig. 1).

The specifications of beam are given in Table 1.

The beam was discretized to planar elements with two degrees of freedom (DOFs) at each node, one deflection and one rotation, as shown in Fig. 1 (Liu *et al.* 2003). The mass and stiffness

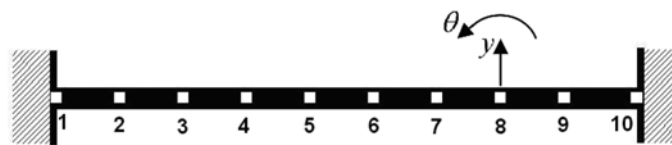


Fig. 1 The model of clamped-clamped beam

Table 1 Specifications of the beam

No. of elements	Young's modulus (Gpa)	Density (kg/m <sup>3</sup> )	Thickness (m)	Width (m)	Length (m)
9	200	7850	0.005	0.038	0.7

matrices of beam were obtained using the equations given in (Liu *et al.* 2003). The natural frequencies and mode shapes of beam were calculated as given in Table 2 and shown in Fig. 3 in below.

### 3.2 Simulation of operational modal analysis

The simulated operational modal testing was conducted by exciting the beam using random excitation. The PSD matrices of the responses were calculated and decomposed to singular values and singular vectors. The singular values spectrum of system is shown in Fig. 2.

The peaks of the first singular value of the system correspond to the natural frequencies and the corresponding singular vectors are the mode shapes of the beam according to explanations in section 2-1. The natural frequencies and mode shapes from FDD are given in Table 2 and Fig. 3.

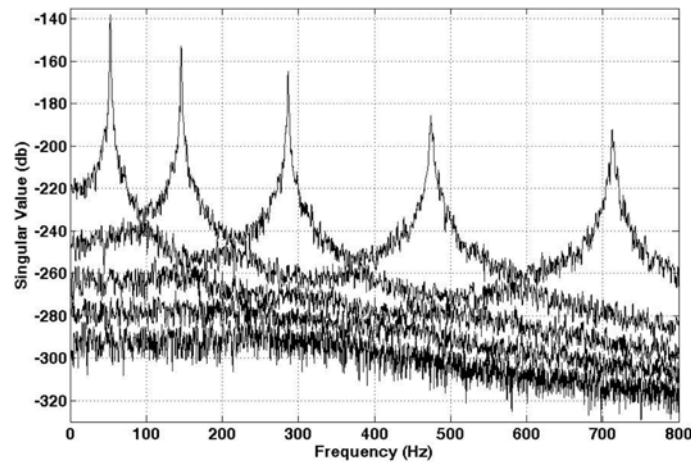


Fig. 2 Singular value spectrums of the clamped-clamped beam under random excitation

Table 2 Comparison of natural frequencies of the beam

Mode #	FEM Natural Freq. - (Hz)	FDD Natural Freq. - (Hz)	Error %
1	53.30	52.79	0.285
2	145.18	146.02	0.019
3	286.63	286.40	0.042
4	474.12	474.70	0.025
5	713.01	712.43	0.011
			Average of Error = 0.076%

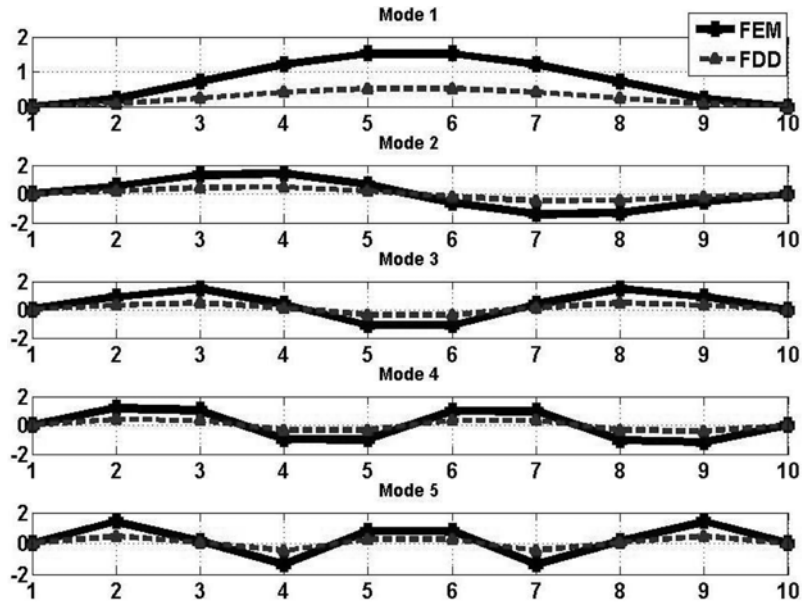


Fig. 3 Comparison of the mode shapes of the beam

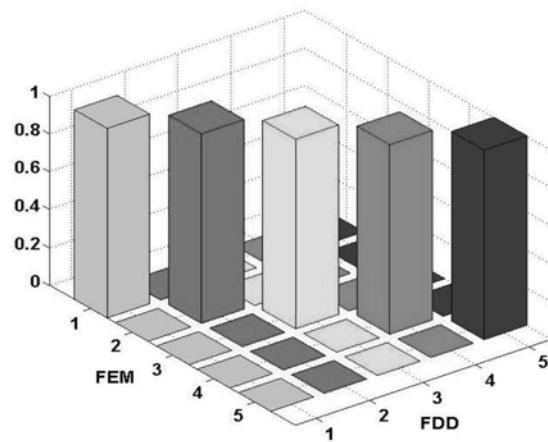


Fig. 4 MAC criteria between FDD and FEM mode shapes

Table 2 shows that FDD can accurately predict the natural frequencies. But the mode shapes are different from those of FE mode shapes (Fig. 3). The mode shapes from FDD and FEM are compared in Fig. 4, based on MAC criterion which is defined as

$$MAC(i,j) = \frac{|\{\varphi\}_{FDD-i}^t \{\varphi\}_{FEM-j}|}{|\{\varphi\}_{FDD-i}^t \{\varphi\}_{FDD-i}| \times |\{\varphi\}_{FEM-j}^t \{\varphi\}_{FEM-j}|} \quad (36)$$

where  $\{\varphi\}_{FDD-i}$  is the  $i^{th}$  FDD mode shape and  $\{\varphi\}_{FEM-j}$  is the  $i^{th}$  FE mode shape.

Fig. 4 shows that the mode shapes obtained from FDD and FEM are completely correlated,



Fig. 5 Beam with added masses

although the FDD mode shapes are not scaled. This means that the mode shapes from FDD can be scaled by applying scaling factors.

### 3.3 Scaling of mode shape using mass change method

The new method was applied to the model of beam and the optimum amount of mass change was computed using Eq. (35) (Fig. 5).

The simulated test was repeated and the scaling factors were calculated and the mode shapes were scaled. Also, the amount of mass change was selected arbitrarily and the mode shapes were scaled. The scaling error was computed using the following equation

$$Error_i = \left| 1 - \frac{\{\varphi\}_{S-i}^t \{\varphi\}_{S-i}}{\{\varphi\}_{F-i}^t \{\varphi\}_{F-i}} \right| \quad (37)$$

where  $\{\varphi\}_{S-i}$  is the  $i^{\text{th}}$  scaled mode shape and  $\{\varphi\}_{F-i}$  is the  $i^{\text{th}}$  FE mode shape including only the translational DOFs. The average and the maximum error of scaling were computed as shown in Table 3.

Table 3 indicates the average and the maximum error of scaling for different amount of the mass change and the optimum mass change calculated from Eq. (35). The errors for the optimum mass change versus each mode are given in Fig. 6. Furthermore, the scaled mode shapes using optimum mass change are shown in Fig. 7. The results show that the proposed formula can minimize the maximum and average error of scaling.

Table 3 Scaling Error for different amount of mass change

No.	$\Delta M_i(\text{gr})$ $i = 1, 2, \dots, 8$	No. of Modes	Max of frequency shift %	Average of Error %	Max of Error %
1	3.4	5	1.54	5.40	8.49
2	8.5	5	3.63	2.15	5.18
3	10.3	5	4.40	1.59	2.65
4	13.7	5	5.66	1.19	2.92
5	17.2	5	6.94	1.00	2.44
6	20.6	5	8.25	0.88	2.87
7	24.1	5	9.50	0.85	1.42
8	31.02	5	11.76	0.62	1.36
Mass change- New Method	28.15	5	10.78	0.50	0.90

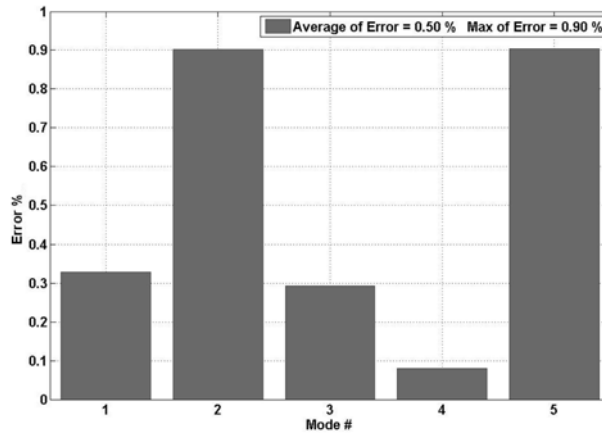


Fig. 6 Error of scaling for optimum mass change

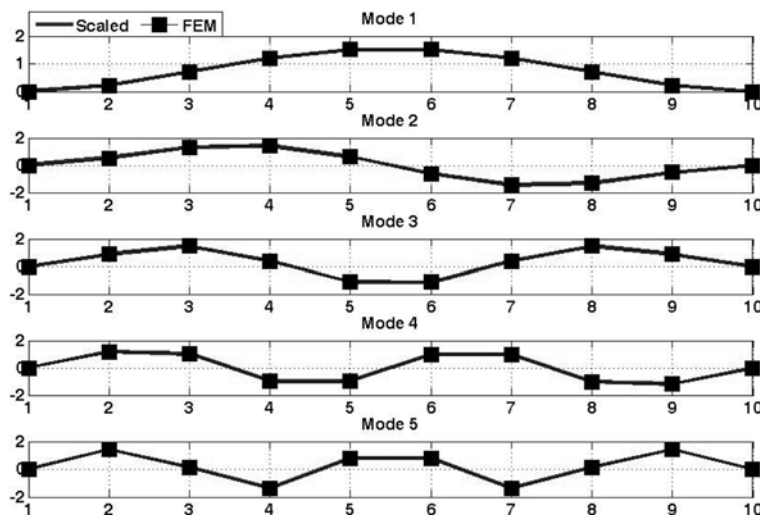


Fig. 7 Comparison of the FE mode shapes and the scaled mode shapes from the optimum mass change

#### 4. Experimental case study

In order to validate the proposed formula a clamped-clamped beam with the same specifications as given in Table 1 was subjected to both an operational modal testing as well as a classical modal testing. As a result the unscaled mode shapes and the correctly scaled mode shapes were estimated.

##### 4.1 Modal testing

A beam was constrained by clamping devices on its both ends as shown in Fig. 8. The specifications of beam are given in Table 1. Eight accelerometers type DJB/A120V were attached to the beam and it was excited by a hammer type BK8202 with the amplifier 2647A (Fig. 8). Grid 3 on the beam was selected for excitation using Modplan software (Modplan 1988-2000). The

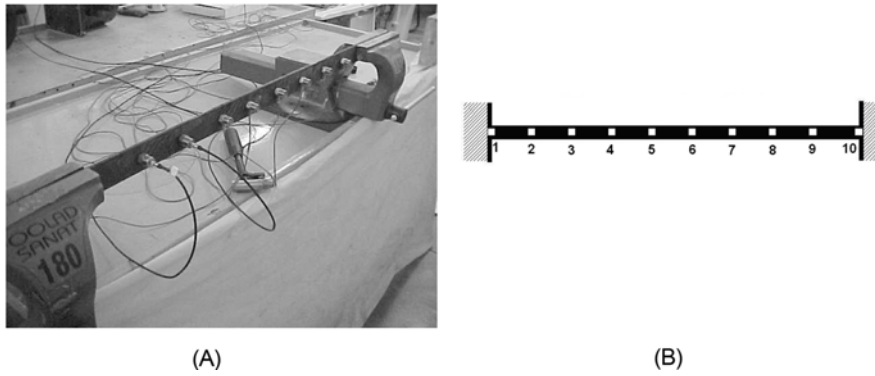


Fig. 8 (A) The clamped-clamped beam subjected to Hammer test and (B) model of clamped-clamped beam

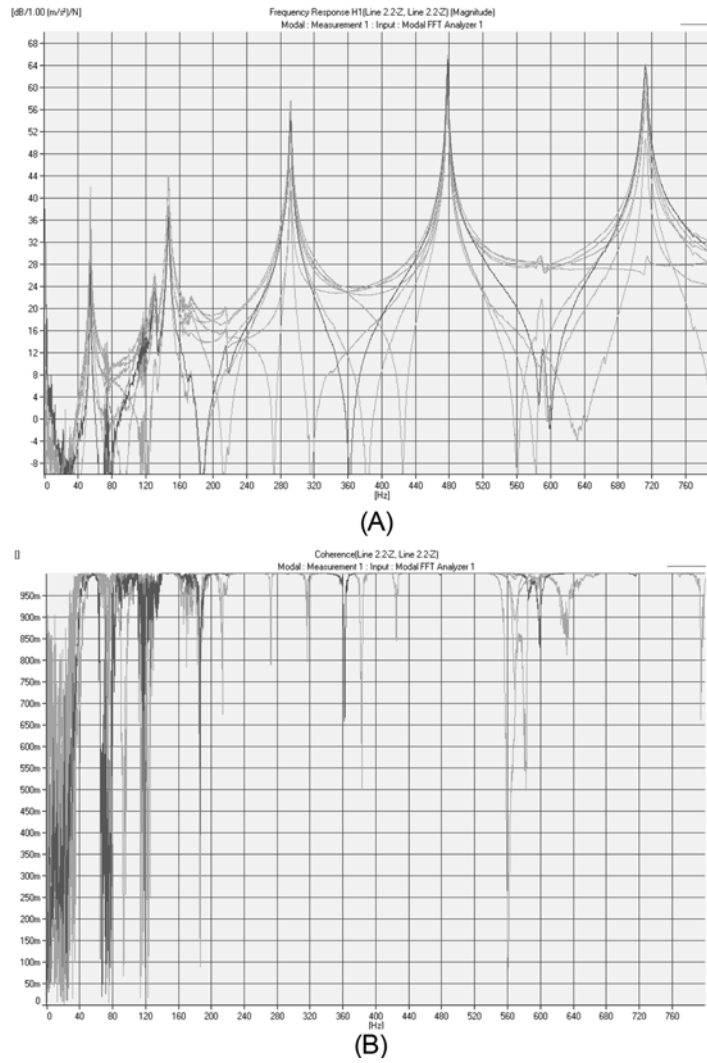


Fig. 9 (A) FRFs from conventional Hammer test, (B) coherences from conventional Hammer test

theoretical relations for the selection of best point for excitation are given in (Imamovic 1998).

The Frequency Response Functions (FRFs) and the coherence functions were calculated (Fig. 9) and the first five natural frequencies (Table 4) and mode shapes (Fig. 11) were obtained.

#### 4.2 Operational modal testing

The operational modal testing consisted of roving hammer impact testing in all points with 8 accelerometers fixed at 8 grid points. The acceleration signals were measured and the FDD method was applied. The PSD matrix of signals was calculated and decomposed to singular values and singular vectors at each frequency. The singular values diagram is shown in Fig. 10.

The first five natural frequencies and unscaled mode shapes of beam were calculated using FDD method. The natural frequencies and mode shapes using conventional modal testing and FDD method are compared in Table 4 and Fig. 11.

Fig. 11 shows that the unscaled mode shapes from FDD method differ from the mode shapes from hammer test. But, the MAC criterion shows the complete correlation between the mode shapes obtained from FDD and those of the hammer test (Fig. 12). This means that the unscaled mode shapes from OMA can be scaled by introducing a scalar number defined as scaling factor.

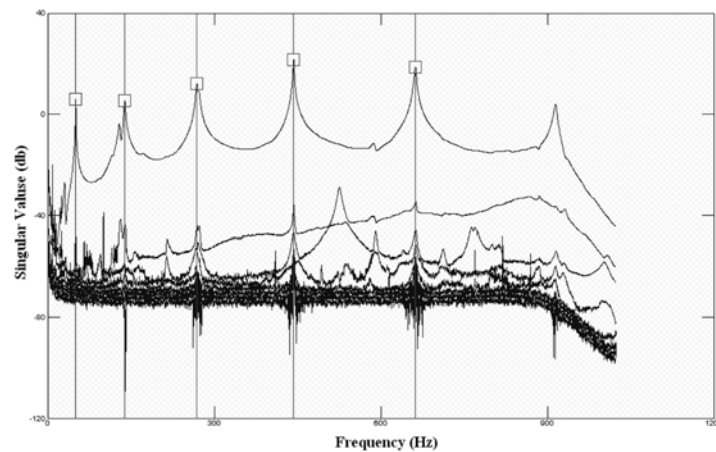


Fig. 10 Singular values spectrum of the beam test from FDD method

Table 4 Comparison of the natural frequencies from FDD and Hammer test

Mode #	Natural Frequency (Hz) Hammer test	Natural Frequency (Hz) OMA test	Error %
1	54.06	54.0	0.115
2	146.59	146.50	0.067
3	291.31	291.25	0.023
4	477.34	477.25	0.020
5	712.07	711.75	0.046
			Average of Error = 0.054%

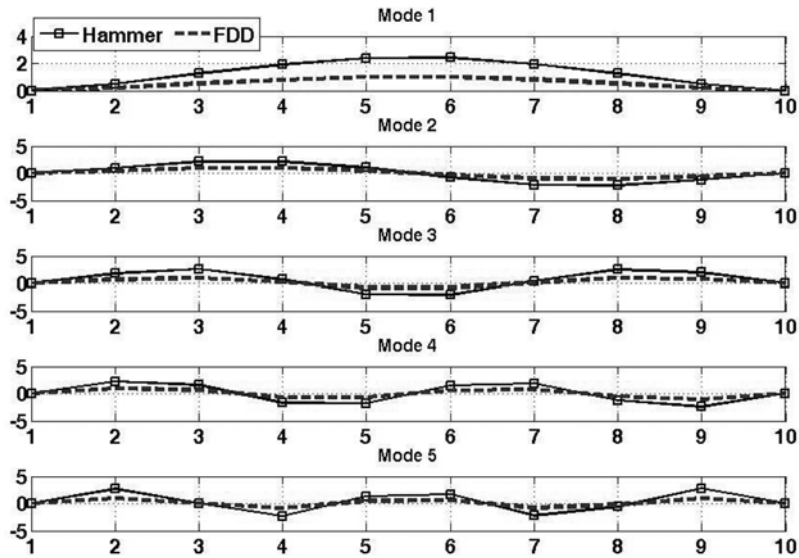


Fig. 11 Comparison of FDD and Hammer mode shapes

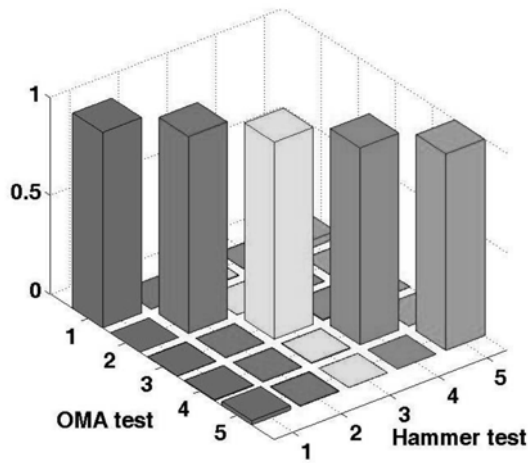


Fig. 12 MAC criterion between FDD and Hammer test mode shapes

### 4.3 Scaling of mode shapes

In order to scale the FDD mode shapes, equal masses were added to the beam at all eight points (Fig. 13). The amounts of added masses were obtained using Eq. (35). Other amounts of added masses were chosen arbitrarily as given in Table 5 for the comparison purposes.

The operational modal test was repeated and the new natural frequencies and mode shapes were obtained and the scaling factors were estimated using Eq. (13) (Table 6).

The mode shapes were compared based on the MSF factor defined as

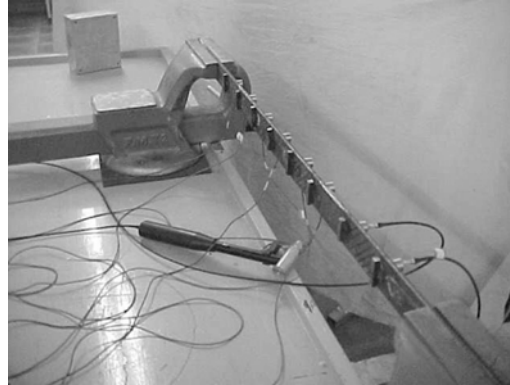


Fig. 13 Addition of masses to the clamped-clamped beam subjected to OMA test

Table 5 The amount of added masses to the beam

Node #	1	2	3	4	5	6	7	8
$\Delta M$ - New Formula (gr)	28.51	28.66	28.92	28.49	28.79	28.55	28.78	28.19
$\Delta M$ - Arbitrary (gr)	8.73	8.97	8.85	8.95	8.92	9.05	8.77	8.57

Table 6 Natural frequencies and Scaling factors of the beam for different added masses

Mode #	1	2	3	4	5
OMA test Freq. (Hz) - (Mass Change – New formula)	50	138.5	268.25	442.75	662.25
OMA test Freq. (Hz) - (Mass Change – Arbitrary)	52.5	140.25	276.75	454.5	682.75
Scaling Factor - New Formula	2.423	2.108	2.693	2.697	2.713
Scaling Factor - Arbitrary	7.015	3.346	2.865	2.916	2.922

Table 7 MSF factors of scaled mode shapes

Mode #	1	2	3	4	5
MSF factor (Mass Change – New Formula)	1.0147	0.9036	1.0599	1.2535	0.9357
MSF factor (Mass Change - Arbitrary)	0.7409	0.9339	0.7303	1.1799	0.8155

$$MSF_i = \frac{\{\varphi\}_{Scaled-i}^t \{\varphi\}_{Scaled-i}}{\{\varphi\}_{Hammer-i}^t \{\varphi\}_{Hammer-i}} \quad (38)$$

where  $\{\varphi\}_{Scaled-i}$  is the  $i^{th}$  scaled mode shape and  $\{\varphi\}_{Hammer-i}$  is the  $i^{th}$  hammer test mode shape.  $MSF$  factor shows how much the scaled mode shapes are correlated to the hammer mode shapes. If the unscaled mode shapes were scaled accurately, the  $MSF$  factors are equal to 1. Table 7 shows the

Table 8 Error of scaling for optimized and arbitrary masses

Mode #	Error (%) - New Formula	Error (%) - Arbitrary
1	1.46	25.91
2	9.63	6.60
3	5.99	26.97
4	25.34	17.99
5	6.42	18.44
Average of Error =9.768%		Average of Error =19.186%

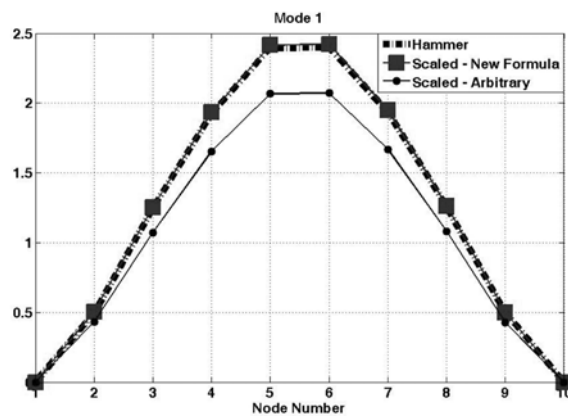


Fig. 14 Comparison of the first mode shape of the clamped - clamped beam

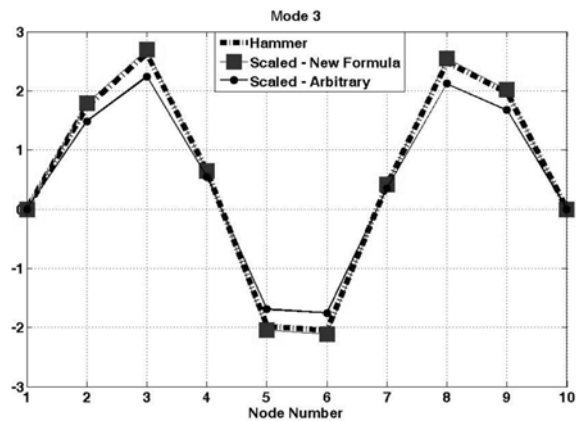


Fig. 15 Comparison of the third mode shape of the clamped - clamped beam

comparison of the *MSF* factors of the scaled mode shapes.

The total error based on Eq. (37) were calculated for both set of mode shapes and compared as shown in Table 8. The average error of the scaled mode shapes using new formula is less than the scaled mode shapes using arbitrary masses although the error for some mode shapes is less for arbitrary masses.

Figs. 14 and 15 show that the first and third scaled mode shapes from both new formula and arbitrary mass change.

## 5. Conclusions

In this paper, a new formula for selection of the magnitude of mass for scaling of OMA mode shapes has been introduced. A priori knowledge of the mode shapes from Finite Element analysis is required for selecting of the optimum added mass. The method was numerically applied to a clamped-clamped beam. The results show that the average error of scaled mode shapes is minimized when the optimum mass change is used. The method was validated experimentally by testing a clamped-clamped beam.

## Acknowledgements

This work is supported by the talented office of Semnan University.

## References

- Abel-Ghaffer, A.M. and Housner, G.W. (1978), "Ambient vibration test of suspension bridge", *Int. J. Eng. Mech. Div.*, **104**(EM5), 983-999.
- Aenlle, M.L., Brincker, R. and Canteli, A.F. (2005a), "Some methods to determine scaled mode shapes in natural input modal analysis", *Proceedings of the 23rd International Modal Analysis Conference (IMAC)*, Florida, February.
- Aenlle, M.L., Brincker, R., Canteli, A.F. and Villa, L.M. (2005b), "Scaling factor estimation by the mass change method", *Proceedings of the 1st International Operational Modal Analysis Conference (IOMAC)*, Copenhagen, April.
- Aenlle, M.L., Fernández, P., Brincker, R. and Canteli, A.F. (2010), "Scaling factor estimation using an optimized mass-change strategy", *Mech. Syst. Signal Pr.*, **24**(5), 1260-1273.
- Asmussen, J.C., Brincker, R. and Rytter, A. (1999), "Ambient modal testing of the VESTVEJ bridge using random decrement", *Proceedings of the 17th International Modal Analysis Conference (IMAC)*, Florida, January.
- Begg, R.D., Mackenzie, A.C., Dodds, C.J. and Loland, O. (1976), "Structural integrity monitoring using digital processing of vibration signals", *Proceedings of the Offshore Technology Conference (OTC)*, Houston, May.
- Bernal, D. (2004), "Modal scaling from known mass perturbation", *J. Eng. Mech.*, **130**(9), 1083-1088.
- Brincker, R. and Andersen, P. (2003), "A way of getting scaled mode shapes in output only modal analysis", *Proceedings of the 21st International Modal Analysis Conference (IMAC)*, Florida, February.
- Brincker, R., Ventura, C. and Andersen, P. (2001a), "Damping estimation by frequency domain decomposition", *Proceedings of the 19th International Modal Analysis Conference (IMAC)*, Florida, February.
- Brincker, R., Zhang, L. and Andersen, P. (2000), "Modal identification from ambient responses using frequency domain decomposition", *Proceedings of the 18th International Modal Analysis Conference (IMAC)*, Florida, February.
- Brincker, R., Zhang, L. and Andersen, P. (2001b), "Modal identification of output only systems using frequency domain decomposition", *Int. J. Smart Mater. Struct.*, **10**(3), 441-445.
- Brownjohn, J.M.W., Magalhaes, F., Caetano, E. and Cunha, A. (2010), "Ambient vibration re-testing and operational modal analysis of the Humber Bridge", *Eng. Struct.*, **32**(8), 2003-2018.
- Coppotelli, G. (2009), "On the estimate of the FRFs from operational data", *Mech. Syst. Signal Pr.*, **23**(2), 288-299.
- Deweert, J. and Dierckx, B. (1999), "Obtaining a scaled modal model of panel type structures using acoustic excitation", *Proceedings of the 17th International Modal Analysis Conference (IMAC)*, Florida, January.
- Doebling, S.W. and Farrar, C.R. (1996), "Computation of structural flexibility for bridge health monitoring using ambient modal data", *Proceedings of the 11th ASCE Engineering Mechanics Conference*, Florida, May.
- Ewins, D.J. (2000), *Modal Testing: Theory, Practice and Application*, Research Studies Press Ltd.
- Hanson, D. (2006), "Operational modal analysis and model updating with a cyclostationary input", Ph.D. Thesis, University of New South Wales.
- Imamovic, N. (1998), "Validation of large structural dynamics models using modal test data", Ph.D. Thesis, Imperial College of Science, Technology & Medicine.
- James, G.H., Crane, T.G. and Laufer, J.P. (1995), "The natural Excitation Technique (NexT) for modal parameter extraction from operating structures", *Int. J. Anal. Exp. Modal A.*, **10**(4), 260-277.
- Khatibi, M.M., Ashory, M.R. and Malekjafarian, A. (2009), "Scaling of mode shapes using mass-stiffness change method", *Proceedings of the 3rd International Operational Modal Analysis Conference (IOMAC)*, Ancona, May.
- Liu, G.R. and Quek, S.S. (2003), *The Finite Element Method: A Practical Course*, Butterworth-Heinemann.

- Modplan (1988-2000), *Integrated Software for Structural Dynamics*, ICATS, Imperial College of Science, Technology and Medicine, University of London, UK.
- Parloo, E. (2003), "Application of frequency – domain system identification techniques the field of operational modal analysis", Ph.D Thesis, Vrije University .
- Parloo, E., Verboven, P., Guillaume, P. and Van Overmeire, M. (2002), "Sensitivity- based operational mode shape normalization", *Mech. Syst. Signal Pr.*, **16**(5), 757-767.
- Randall, R.B., Gao, Y. and Swevers, J. (1998), "Updating modal models from response measurements", *Proceedings of the 23rd International Conference on Noise and Vibration Engineering (ISMA23)*, Leuven, September.
- Wenzel, H. and Pichler, D. (2005), *Ambient Vibration Monitoring*, John Wiley & Sons Ltd.
- Zhang, L., Brincker, R. and Andersen, R. (2005), "An overview of operational modal analysis: major development and issues", *Proceedings of the 1st International Operational Modal Analysis Conference (IOMAC)*, Copenhagen, April.